Selkov Dynamic System with Variable Heredity for Describing Microseismic Regimes

Roman Parovik

Institute of Cosmophysical Research and Radio Wave Propagation FEB RAS

September 27, 2023

Introduction

Microseisms are vibrations of the earth's surface of small amplitude, which occur as a result of natural and man-made processes. For example, natural processes can be associated with the processes of formation and passage of cyclones in the atmosphere, with the processes of the impactof seas and oceans on the coast. Technogenic processes associated with human activities, for example, the construction of buildings and structures, traffic, the operation of power plant engines, etc.

The condition for the occurrence of microseisms is determined by the presence of elasticity of the medium, the ability to accumulate stress to a certain critical value, and on the other hand, the presence of fragility - the ability to collapse under the action of forces, the level of which is noticeably lower than the yield point [1]. The fragility of the medium is realized at the macroscopic level due to the appearance and growth of the length of cracks. The process of multiple crack formation ends with the destruction of the medium. In this article, we study the process of crack formation at an early stage of failure.

Introduction

Note that the growth of the crack length may slow down with time, and if the medium has viscosity, then the crack length can also decrease until it is completely closed. In [2], the authors believe that such a process can occur in the earth's crust at great depths at high pressure and temperature. Under such conditions, a diffusion process occurs in the crack tips, which leads to their tightening.

According to the terminology of [2], there are two types of microseisms: regular weak oscillations with periods from 2 to 10 s and less regular ones with long periods of oscillations up to 30 s. The first type of microseisms are excited by cracks of small length, which cannot be recorded by seismic equipment. We will call such cracks trigger or tr-cracks, which are triggers for larger cracks. Microseismic signals of the second type are generated by longer fractures, which are already registered by seismic equipment. We will call such cracks gs-cracks.

Introduction

Next, we will investigate the mechanism of self-oscillations microseismic sources or fluctuations in the concentration of gs-fractures, by analogy with [2]. The self-oscillatory process here consists in the interaction of tr-cracks and gs-cracks, which is shown in Fig.1.

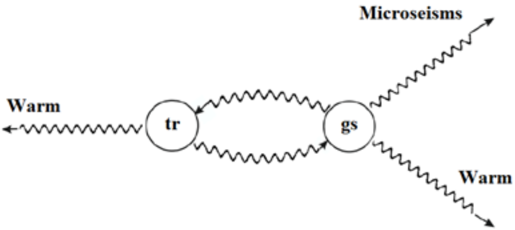

Figure 1. Self-oscillatory process in the interaction between tr-cracks and gs-cracks [2]

Trigger tr-cracks are seed cracks with lower energy, and when the critical level is reached, the concentration transforms into gs cracks. Further, according to the Le Chatelier-Brown principle [3], gs-cracks that generate microseismic signals partially disappear after energy release, and partially turn into tr-cracks. Further, the process of interaction is repeated, and a self-oscillatory regime occurs.

In the article [2], the authors proposed to use the Selkov nonlinear dynamic system to describe the self-oscillating process of interaction of tr and gs-cracks in an elastic-brittle medium. The Selkov dynamic system studied in biology when modeling self-oscillatory modes of substrates and glycolysis products [4]. The article [2] studies the equilibrium points of the Selkov dynamic system in order to determine the conditions for the existence of undamped oscillations. Spectra of microseismic oscillations are also studied.

Introduction

A generalization of the results in the article [2] is a series of works by the author [5], [6], in which the memory effects in a self-oscillatory system were taken into account. The memory effect determines the dependence of the current state of an oscillatory (dynamic) system on its previous states. From the point of view of mathematics, the memory effect can be described using integro-differential equations, in particular, using fractional derivatives. A dynamical system with derivatives of fractional orders will be called a fractional dynamical system.

In [6] the Selkov fractional dynamical system was studied, a numerical solution algorithm based on the Adams-Bashfort-Multon method was proposed, the stability and convergence of the method were studied, and test examples were given. In [5] the qualitative properties of the Selkov fractional dynamical system were studied, regular and chaotic regimes were studied. It is shown that a dynamic system can have different regimes, including chaotic ones.

In this article, we continue to study the fractional Selkov dynamical system in the case when the derivatives have fractional variable orders in time. A numerical algorithm for solving the solution is proposed, the simulation results were visualized in the Maple computer mathematics environment, oscillograms and phase trajectories were constructed for cases where the orders of fractional derivatives are monotonic functions of time, as well as periodic functions of time.

Consider the following nonlinear dynamical system:

$$\begin{cases} \partial_{0t}^{\alpha_1(t)} x(t) = -x(t) + ay(t) + bx^2(t)\,y(t),\, x(0) = x_0 \\ \partial_{0t}^{\alpha_2(t)} y(t) = v - ay(t) - bx^2(t)\,y(t),\, y(0) = y_0. \end{cases} \quad (1)$$

where $x(t) \in C^1[0, T]$ is a function that determines the concentration of tr-cracks; $y(t) \in C^1[0, T]$ is a function that determines the concentration of gs-cracks that generate microseisms, $t \in [0, T]$ is the coordinate responsible for the current time of the process, T is a constant, simulation time; x_0, y_0, v, a, b - given positive constants; fractional differentiation operators are understood in the sense of the Gerasimov-Caputo orders $0 < \alpha_1(t), \alpha_2(t) < 1$ and are determined according to [7].

$$\begin{aligned} \partial_{0t}^{\alpha_1(t)} x(t) &= \frac{1}{\Gamma(1-\alpha_1(t))} \int_0^t \frac{\dot{x}(\tau)\,d\tau}{(t-\tau)^{\alpha_1(t)}}, \\ \partial_{0t}^{\alpha_2(t)} y(t) &= \frac{1}{\Gamma(1-\alpha_2(t))} \int_0^t \frac{\dot{y}(\tau)\,d\tau}{(t-\tau)^{\alpha_2(t)}}. \end{aligned} \quad (2)$$

We will assume that the functions $\alpha_1(t), \alpha_2(t) \in C(0, 1)$.

Problem statement and solution technique

The dynamical system (1) will be called a fractional Selkov dynamical system with variable memory. In the works of the author [5], [6] the fractional Selkov dynamical system was considered, when the fractional orders of the derivatives are constant: $\alpha_1(t) = \alpha_1, \alpha_2(t) = \alpha_2$.

The properties of fractional derivatives of constant order are described in detail in the books [8]–[10]. In the case when $\alpha_1 = \alpha_2 = 1$, then we get the classical Sel'kov dynamical system [4].

To study the Selkov fractional dynamical system (SFDS) (1), we use the Adams-Bashforth-Moulton (ABM) numerical method from the family of predictor-corrector methods. The ABM method has been studied and discussed in detail in [11], [12]. We adapt this method to solve SFDS (1).

Problem statement and solution technique

To do this, we use Definitions 2, and on a uniform grid with step we introduce the functions x^p_{n+1}, y^p_{n+1}, $n = 0, ..., N-1$, which will be determined by the Adams-Bashforth formula (predictor):

$$\begin{cases} x^p_{n+1} = x_0 + \dfrac{\tau^{\alpha_{1,n}}}{\Gamma\left(\alpha_{1,n}+1\right)} \sum\limits_{j=0}^{n} \theta^1_{j,n+1} \left(-x_j + ay_j + bx_j^2 y_j\right), \\ y^p_{n+1} = y_0 + \dfrac{\tau^{\alpha_{2,n}}}{\Gamma\left(\alpha_{2,n}+1\right)} \sum\limits_{j=0}^{n} \theta^2_{j,n+1} \left(v - ay_j - bx_j^2 y_j\right), \\ \theta^i_{j,n+1} = (n-j+1)^{\alpha_{i,n}} - (n-j)^{\alpha_{i,n}}, i = 1, 2, \end{cases} \tag{3}$$

as well as functions x_{n+1}, y_{n+1}, which will be determined by the Adams-Moulton formula for the corrector:

$$\begin{cases} x_{n+1} = x_0 + \dfrac{\tau^{\alpha_{1,n}}}{\Gamma\left(\alpha_{1,n}+2\right)} \times \\ \times \left(\left(-x^P_{n+1} + ay^P_{n+1} + b\left(x^P_{n+1}\right)^2 y^P_{n+1} \right) + \sum\limits_{j=0}^{n} \rho^1_{j,n+1} \left(-x_j + ay_j + bx_j^2 y_j\right) \right), \\ y_{n+1} = y_0 + \dfrac{\tau^{\alpha_{2,n}}}{\Gamma\left(\alpha_{2,n}+2\right)} \times \\ \times \left(v - ay^P_{n+1} - b\left(x^P_{n+1}\right)^2 y^P_{n+1} + \sum\limits_{j=0}^{n} \rho^2_{j,n+1} \left(v - ay_j - bx_j^2 y_j\right) \right), \end{cases} \tag{4}$$

where the weight coefficients in (4) are determined by the formula:

$$\rho^{i}_{j,n+1} = \begin{cases} n^{\alpha_{i,n}+1} - (n-\alpha_{i,n})(n+1)^{\alpha_{i,n}} & ,j=0, \\ (n-j+2)^{\alpha_{i,n}+1} + (n-j)^{\alpha_{i,n}+1} - 2(n-j+1)^{\alpha_{i,n}+1}, & 1 \le j \le n, \\ 1, & ,j=n+1, \\ i=1,2. \end{cases}$$

Remark 1. *It is known that for the ABM method the error estimate is valid [13]*:

$$\max_{1\le j\le k} \left|x_i\left(t_j\right) - x_{i,j}\right| = O\left(\tau^{\min\left(2,1+\alpha_{i,m}\right)}\right),$$

$$\alpha_i = \min_{0<\tau<T} \alpha_i\left(\tau\right), x_1\left(t_j\right) = x\left(t_j\right), x_2\left(t_j\right) = y\left(t_j\right), i=1,2.$$

Remark 2. *Note that in the classical case $\alpha_i = 1$, we obtain the classical ABM method of the second order of accuracy.*

Next, using specific examples, we consider various cases when the functions $\alpha_i\left(t\right)$ are monotonic, as well as periodic.

The implementation of the numerical algorithm (3)-(4) was carried out using the Maple package.

Example 1. *The case of linearly monotonically decreasing functions $\alpha_i(t)$ (Fig. 1):*

$$\alpha_1(t) = 0.8 - 0.01\frac{t}{T}, \alpha_2(t) = 0.9 - 0.02\frac{t}{T}.$$

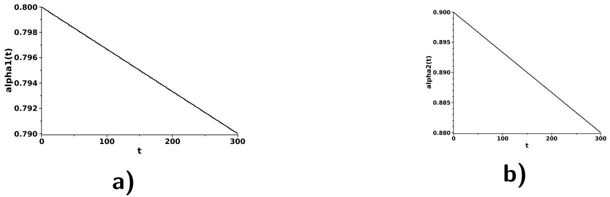

Figure 2. a) $\alpha_1(t)$; b) $\alpha_2(t)$ for Example 1

We take the remaining parameters for system (1) as follows:

$$v = 0.6, a = 0.03, b = 1.3, x(0) = 1, y(0) = 0.5.$$

For the numerical algorithm (3)-(4), the parameters have the following meanings: $N = 2000$, $T = 300, \tau = 0.15$.

Results

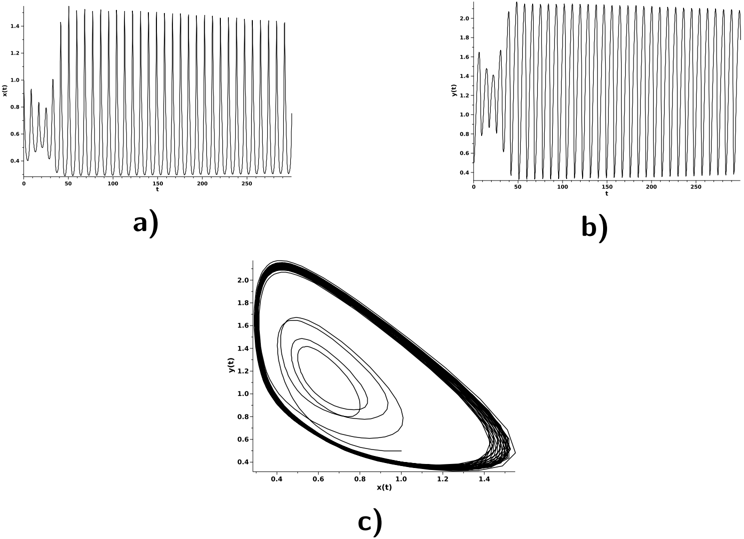

Figure 3. Osillograms: a) fluctuations in the concentration of tr-cracks; b) fluctuations in the concentration of gs-cracks. Phase trajectory c)

Figure 3 shows that in the case when the functions $\alpha_1(t), \alpha_2(t)$ are monotonically decreasing, then the concentration of trigger cracks and the concentration of cracks generating microseisms eventually reach a constant level. The phase trajectory is a trajectory characteristic of the limit cycle.

An important task is the study of limit cycles, in particular, their stability. According to the definition of limit cycle stability, there must exist an ε neighborhood such that all phase trajectories that start in this neighborhood approach the limit cycle asymptotically at $t \to \infty$.

Based on the above, we will construct a phase trajectory for Example 1 in the case when the initial conditions have other values (Fig. 3): $x(0) = y(0) = 1.5$.

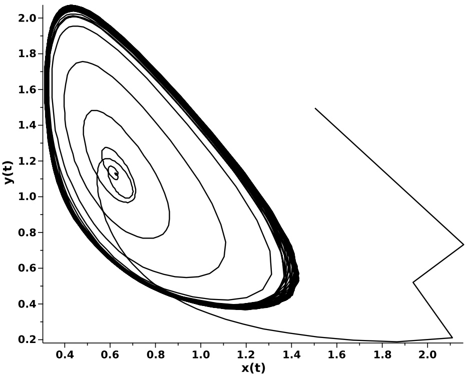

Figure 4. Phase trajectory for $x(0) = y(0) = 1.5$

We see that the phase trajectory is approaching a limit cycle to the same as in Fig. 4. We see on that the phase trajectory is approaching the limit cycle to the same one as in Fig. 3c.

Therefore, we can say about the possible stability of the limit cycle. For an affirmative answer to this question, it is necessary to substantiate a theorem analogous to the Poincare-Bendixson theorem for the case of fractional dynamical systems.

The author's work [6] shows that the limit cycle disappears as $\alpha_1 = 0.5$ tends. Further, the oscillatory process disappears. Let Fig. 5

$$\alpha_1(t) = 0.8 - 0.3\frac{t}{T}, \alpha_2(t) = 0.9 - 0.4\frac{t}{T}.$$

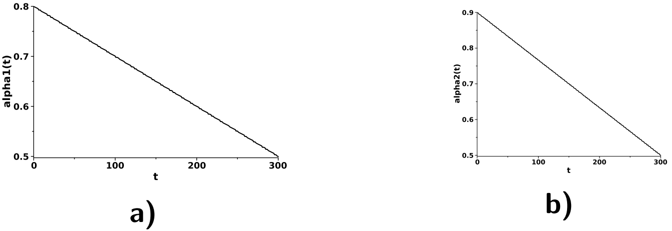

Figure 5. a) $\alpha_1(t) \in [0.5, 0.8]$; b) $\alpha_2(t) \in [0.5, 0.9]$ for Example 1

Results

The rest of the parameters will be left unchanged.

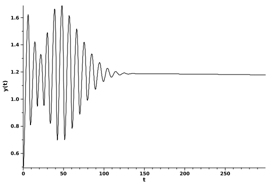

a)

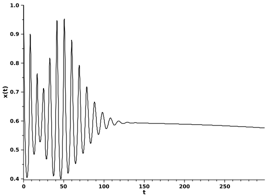

b)

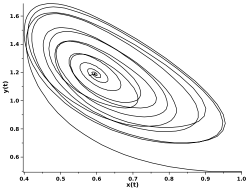

c)

Figure 6. Osillograms: a) fluctuations in the concentration of tr-cracks; b) fluctuations in the concentration of gs-cracks. Phase trajectory c)

From Fig. 6 it can be concluded that, as the values of the functions $\alpha_1(t), \alpha_2(t)$ decrease to 0.5, the oscillations decay. It can be given from Fig. 5 an approximate estimate from which oscillations begin to decay: $\alpha_1 \approx 0.675, \alpha_2 \approx 0.675$.

Let us expand the range of variation of the functions $\alpha_1(t) \in [0.2, 1], \alpha_2(t) \in [0.3, 1]$.

The rest of the parameters will remain unchanged.

$$\alpha_1(t) = 1 - 0.8\frac{t}{T}, \alpha_2(t) = 1 - 0.7\frac{t}{T}.$$

The simulation results are shown in Fig. 7.

Results

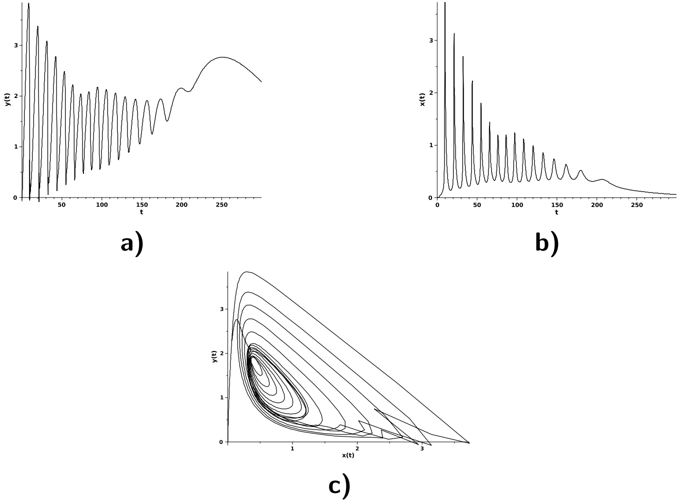

Figure 7. Osillograms: a) fluctuations in the concentration of tr-cracks; b) fluctuations in the concentration of gs-cracks. Phase trajectory c)

Here we can see several modes: reaching the limit cycle, damped mode and aperiodic mode.

Example 2. *The case of periodic functions* $\alpha_i(t)$ Fig. 8:

$$\alpha_1(t) = 0.9 - \frac{5\cos(0.3\pi t)}{T}, \alpha_2(t) = 0.9 - \frac{7\sin(0.2\pi t)}{T}.$$

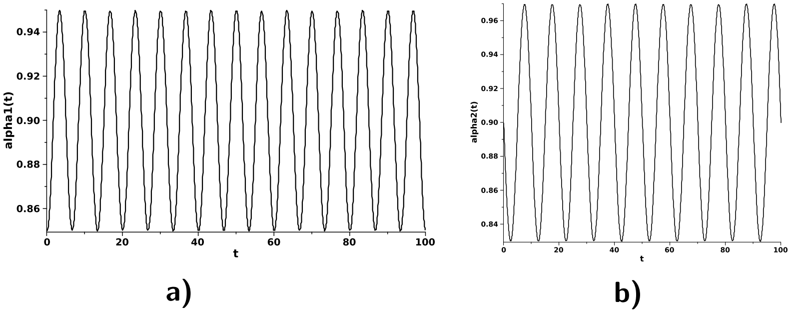

Figure 8. a) $\alpha_1(t)$; b) $\alpha_2(t)$ for Example 2

We take the remaining parameters for system (1) as follows: $v = 0.6, a = 0.03, b = 1.3, x(0) = 0.01, y(0) = 0.054$. For the numerical algorithm (3)-(4), the parameters have the following meanings: $N = 3000$, $T = 300, \tau = 0.1$.

The simulation results are shown in Fig. 9. From Fig. 9, we see that the oscillograms (Fig. 9a, b) have a multiperiodicity, which is also reflected in the phase trajectory (Fig. 9c). The presence of loops, self-crossings is typical for oscillatory processes with memory. Such regimes may indicate the presence of chaotic regimes.

Results

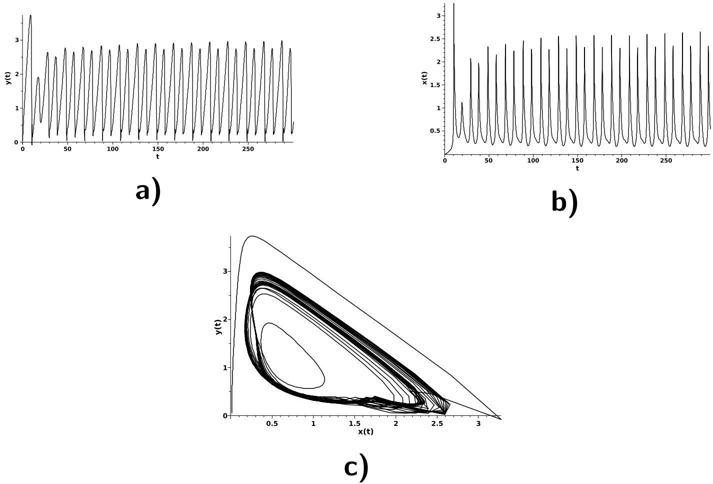

Figure 9. Osillograms: a) fluctuations in the concentration of tr-cracks; b) fluctuations in the concentration of gs-cracks. Phase trajectory c)

Example 3. *The case of periodic functions $\alpha_i(t)$* (Fig. 10):

$$\alpha_1(t) = 1 - \frac{15\exp(\cos(0.4\pi t))}{T}, \alpha_2(t) = 1 - \frac{13\exp(\sin(0.4\pi t))}{T}.$$

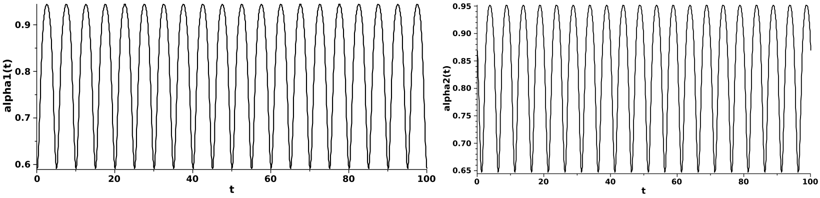

a) **b)**

Figure 10. a) $\alpha_1(t) \in [0.6, 0.9]$; b) $\alpha_2(t) \in [0.65, 0.95]$ for Example 3

We take the remaining parameters for system (1) as follows: $v = 0.6, a = 0.03, b = 1.3, x(0) = 1, y(0) = 1$.

For the numerical algorithm (3)-(4), the parameters have the following meanings: $N = 2000$, $T = 100, \tau = 0.05$.

Results

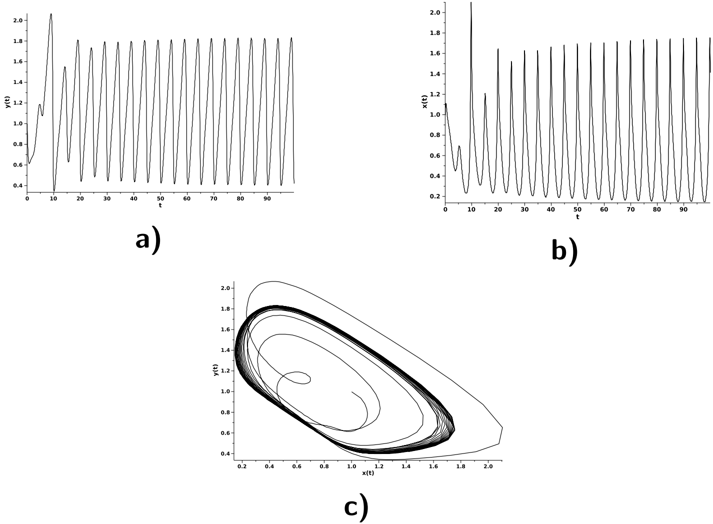

Figure 11. Osillograms: a) fluctuations in the concentration of tr-cracks; b) fluctuations in the concentration of gs-cracks. Phase trajectory c)

Results

It can be seen here (Fig.11c) that a more complex form of the functions $\alpha_1(t)$ and $\alpha_2(t)$ can lead to limit cycles of a different form than those previously known.

Let's expand the range of functions $\alpha_1(t) \in [0.2, 0.8], \alpha_2(t) \in [0.2, 0.8]$ as in the previous examples:

$$\alpha_1(t) = 1 - \frac{30\exp(\cos(0.4\pi t))}{T}, \alpha_2(t) = 1 - \frac{30\exp(\sin(0.4\pi t))}{T}.$$

Let's see how the phase trajectory and oscillograms change compared to Fig.11.

We see that the phase trajectory in Fig.12c differs from the phase trajectory in Fig. 11c. Here the phase trajectory and the limit cycle have a more complex form. It should also be noted that the phase trajectory reaches the limit cycle faster.

Results

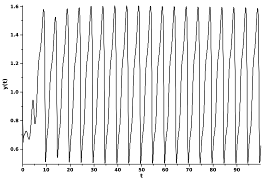

a)

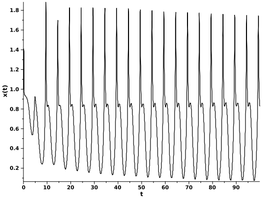

b)

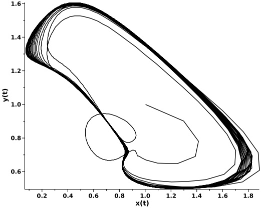

c)

Figure 12. Osillograms: a) fluctuations in the concentration of tr-cracks; b) fluctuations in the concentration of gs-cracks. Phase trajectory c)

Conclusion

The results of the work show the following taking into account the effects of memory in oscillatory systems using derivatives of fractional variable orders allows for more flexible mathematical modeling. If the orders of fractional derivatives are linearly decreasing functions, then we can observe several modes: reaching the limit cycle, damped and aperiodic. Approximate estimates of the transition or bifurcation from one regime to another were given in the work. If the orders are periodic functions, then multiperiodic regimes, limit cycles of various shapes can arise, which indicates a very rich dynamics of the process. Due to the fact that it is important for us to study the self-oscillatory regime, which is characterized by a limit cycle, further continuation of the work is connected with the study of its stability.

Conclusion

Another line of work is the study of chaotic regimes. Due to the fact that the methodology of works [14] is not applicable to the study of dynamic systems of fractional variable order, it is necessary to use approaches related to the construction of maps of dynamic modes [15]. This approach requires large computational resources, as well as the methodology of parallelization of numerical algorithms.

This research was funded by Russian Science Foundation grant number 22-11-00064 "Modeling of dynamic processes in geospheres taking into account hereditarity" https://rscf.ru/project/22-11-00064/.

References I

[1] Ph. Kearey. *The Encyclopedia of Solid Earth Sciences*. Hoboken: Blackwell Sci., 1993.

[2] V. I. Makovetsky, I. P. Dudchenko, and A. S. Zakupin. "Auto oscillation model of microseism's sources". In: *Geosistemy perehodnykh zon* 4(1) (2017), pp. 37–46.

[3] O. Shpielberg and E. Akkermans. "Le Chatelier principle for out-of-equilibrium and boundary-driven systems: Application to dynamical phase transitions". In: *Physical review letters* 116.24 (2016), p. 240603. DOI: 10.1103/PhysRevLett.116.240603.

[4] E. E. Selkov. "Self-oscillations in glycolysis. I. A simple kinetic model". In: *Eur. J. Biochem.* 4 (1968), pp. 79–86.

References II

[5] R. I. Parovik, Z. Rakhmonov, and R. Zunnunov. "Study of Chaotic and Regular Modes of the Fractional Dynamic System of Selkov". In: *EPJ Web of Conferences* 254 (2021), p. 02014. DOI: 10.1051/epjconf/202125402014.

[6] R. I. Parovik. "Studies of the Fractional Selkov Dynamical System for Describing the Self-Oscillatory Regime of Microseisms". In: *Mathematics* 10.22 (2022), p. 4208. DOI: 10.3390/math10224208.

[7] S. Patnaik, J.P. Hollkamp, and F. Semperlotti. "Applications of variable-order fractional operators: A review.". In: *R. Soc. A R. Soc. Publ.* 476 (2020), p. 20190498. DOI: 10.1098/rspa.2019.0498.

[8] A.A. Kilbas, H.M. Srivastava, and J.J. Trujillo. *Theory and Applications of Fractional Differential Equations*. Amsterdam: Elsevier, 2006.

References III

[9] K. B. Oldham and J. Spanier. *Theory and applications of differentiation and integration to arbitrary order*. London: Academic Press, 1974.

[10] K. S. Miller and B. Ross. *An introduction to the fractional calculus and fractional differntial equations*. New York: A Wiley-Interscience publication, 1993.

[11] R. Garrappa. "Numerical Solution of Fractional Differential Equations: A Survey and a Software Tutorial". In: *Mathematics* 6.2 (2018), p. 16. DOI: 10.3390/math6020016.

[12] R. Parovik. "Application of the Adams-Bashforth-Moulton method to the numerical study of linear fractional oscillators models". In: *AIP Conference proceedings* 2365 (2021), p. 020006. DOI: 10.1063/5.0056846.

[13] Shichang Ma, Xu Yufeng, and Yue Wei. "Numerical solutions of a variable-order fractional financial system". In: *Journal of Applied Mathematics* 2012 (2012), p. 417942. DOI: 10.1155/2012/417942.

[14] I. Petras. *Fractional Order Nonlinear Systems. Modeling, Analysis and Simulation.* Beijing, Springer-Verlag Berlin Heidelberg: Springer, 2011.

[15] R.I. Parovik and T.P. Yakovleva. "Construction of maps for dynamic modes and bifurcation diagrams in nonlinear dynamics using the Maple computer mathematics software package". In: *Journal of Physics: Conference Series* 2373 (2022), p. 052022. DOI: 10.1088/1742-6596/2373/5/052022.